NANO LETTERS

2005
Vol. 5, No. 12
2394−2398

Evidence of Sequential Lift in Growth of Aligned Multiwalled Carbon Nanotube Multilayers

Mathieu Pinault,[†] Vincent Pichot,[‡] Hicham Khodja,[§] Pascale Launois,[‡] Cécile Reynaud,[†] and Martine Mayne-L'Hermite*[,†]

Laboratoire Francis Perrin (CEA CNRS URA 2453), DSM-DRECAM-SPAM, CEA Saclay, 91191 Gif sur Yvette, France, Laboratoire de Physique des Solides (CNRS UMR 8502), Université Paris Sud, 91405 Orsay, France, and Laboratoire Pierre Süe, CEA-CNRS UMR 9956, CEA Saclay, 91191 Gif sur Yvette, France

Received July 28, 2005

ABSTRACT

We synthesized aligned multiwalled carbon nanotube multilayers by aerosol-assisted catalytic chemical vapor deposition through sequential injections of aerosols containing both carbon and catalyst precursors. Each sequence was traced by a specific duration or precursor mixture, with the carbon source being possibly enriched in ^{13}C isotope labels. We discovered that any sequence involved the growth of a new layer on the substrate surface, under any pre-existing one by lifting it up, giving definitive evidence of a base-growth mechanism.

There has been tremendous progress in the production of carbon nanotubes since their discovery.[1] In particular, aligned multiwalled carbon nanotubes (MWNT) are produced by catalytic chemical vapor deposition (CCVD).[2−11] Two methods can be used. The first one is based on the CVD of gaseous hydrocarbons on catalysts previously deposited on substrates,[2−5] and the growth mechanism is most often identified as a base growth.[4,5] The second one is based on the CVD of solutions containing both a liquid hydrocarbon and a catalyst precursor,[6−11] but the growth mechanisms are not definitely understood. Various models resulting from the analysis of aligned nanotube carpets report contradictory growth processes. Authors report either a base-growth mechanism[10] or a tip-growth mechanism[9] in which CNTs could grow from direct deposition of Fe particles and carbon clusters on their open upper tips or even a competition between base and tip growth.[11] In addition, some studies mentioning the formation of multilayered aligned nanotubes always report the formation of the successive carpets on the top of pre-existing ones without giving any experimental evidence of the progress of carbon during the multilayer formation.[12−15] Only, the same hypothesis on growth from the upper tips is given.[12,15]

This study is focused on the chronology of aligned carbon nanotube growth during an aerosol-assisted CCVD process. We report microscopy analysis, in conjunction with carbon monitoring by isotope labeling, along multilayered aligned carbon nanotubes formed on Si substrates. We show for the fist time that successive layers are always growing under the previous ones by lifting them up. This result demonstrates the involvement of a base-growth mechanism from the substrate surface. In addition, C species are diffusing continuously through the multilayered carpet and subsequently feeding the origin of the nanotube growth located on the surface substrate to form carbon nanotubes that are growing up.

The aerosol-assisted CVD method is based on the catalytic decomposition of liquid hydrocarbons from the pyrolysis of mixed aerosols containing both a hydrocarbon source and a metallic precursor as a catalytic source that fills the reactor volume simultaneously and continuously. The experimental setup is described in details elsewhere.[16,17] Samples of well-aligned MWNTs arranged as in a "carpet" and almost free of any byproducts are obtained on silicon substrates. Typical nanotube carpets (noted sample A in the following) are obtained from pyrolysis of a 5 wt % ferrocene solution in toluene at 850 °C during a 15-min time period.[16,18]

In the present study, a special experimental procedure consisting of sequential injections of hydrocarbon/metallocene aerosol in the hot reactor has been developed (see also Figure S1). The hydrocarbon source is either toluene or benzene, and the metal precursor is ferrocene. The sequential injection is described as successive injections of

* To whom correspondence should be addressed. Phone: +33 1 69 08 48 47. Fax: + 33 1 69 08 87 07. E-mail: mayne@drecam.cea.fr.
[†] Laboratoire Francis Perrin.
[‡] Laboratoire de Physique des Solides.
[§] Laboratoire Pierre Süe.

10.1021/nl051472k CCC: $30.25
Published on Web 11/08/2005

Table 1. Synthesis Conditions for Samples Synthesized by Sequential Injections[a]

sample	aerosol generator	constant conditions	varying parameters during the sequential injections				
			1	2	3	4	5
P1	US generator	T + F (5 wt %)	10 min	10 min	5 min	5 min	5 min
P2	US generator	T + F (5 wt %)	15 min	15 min	20 min		
I1	injection system	T + F	F (2.5 wt %) ~3 min	F (0%) ~12 min			
I2	injection system	T + F	F (2.5 wt %) ~4 min	F (0%) ~4 min	F (2.5 wt %) 5 min	F (2.5 wt %) 5 min	F (2.5 wt %) 10 min
I3	injection system	B + F (2.5 wt %)	B ~7 min 30	B* ~1 min 30	B ~7 min 30	B* ~2 min 30	

[a]T is for toluene, F is for ferrocene, B is for benzene, and B* is for benzene containing ^{13}C isotope labels.

defined durations. Each injection is characterized by the nature of hydrocarbon source and/or ferrocene concentration. The aerosol is generated with either an ultrasonic (US) generator (Pyrosol RBI, France) for successive injections of the same solutions or a motor injection system (Qualiflow-Jipelec, France) for injections of solutions composed of different hydrocarbons and/or ferrocene concentrations. The aerosol is always carried to the hot reactor (850 °C) by an argon flow (1 L/min). Most often, between each successive injection, the aerosol generation is stopped while the Ar flow rate and reactor temperature are maintained during a 10-min time period to ensure that the aerosol is no longer present and thus that the reaction is stopped when the next injection is started.

Different kinds of samples are synthesized according to the different injection sequences (Table 1). The first set of experiments (samples P1 and P2) is performed on silicon substrates with the US generator and consists of successive aerosol injections of different durations using the same toluene/ferrocene (5 wt %) solution. A special sample, P3, was also synthesized by again introducing sample A in the reactor (a typical nanotube carpet, see above) after storage at room temperature and by injecting toluene/ferrocene (5 wt %) aerosol during a 10-min time period in the hot reactor (850 °C). The second set of experiments is achieved with the injection system, which allows sequential injections of different kinds of solutions. Samples I1 and I2 were synthesized on Si substrates from sequential injections of aerosol exhibiting different ferrocene concentrations from 0 (pure toluene aerosol) to 2.5 wt %. Sample I3 was synthesized from benzene/ferrocene solutions. The particularity of this synthesis is the use of ^{13}C-enriched benzene as a carbon source, allowing us to perform sequential injections of either standard benzene/ferrocene or ^{13}C-enriched benzene/ferrocene solution in order to localize carbon containing ^{13}C isotope labels in the final sample. Only for this sample the different sequences were performed continuously without stopping between each sequence. It is important to note that, generally, the durations of the last injections were most often different from the previous ones in order to localize the nanotube growth precisely.

To determine the morphology and size of the sample obtained, the arrangement of the nanotube, and to localize the nanotube growth, we cut samples carefully through their thickness with a razor blade to the silicon substrate. They were then observed by scanning electron microscopy (SEM) (Léo-Gémini, field emission gun). X-ray microdiffraction experiments, with a beam size of $2 \times 2\ \mu m^2$, were performed using high-flux synchrotron radiation at ESRF (beamline ID13, wavelength 0.9755 Å) to analyze the nanotube alignment quantitatively. The small beam size allowed us to analyze it locally from the basis to the top of the sample. Determination of the nanotube orientation around the normal to the substrate is obtained from half-width at half maximum (HWHM) of the angular modulation of (002) MWNT diffraction peak at 1.83 $Å^{-1}$.[19] Sample I3 was analyzed with the nuclear microprobe in Laboratoire Pierre Süe (Saclay, France). The principle is based on the spectrometry of the reaction products induced by the interaction of a deuteron microbeam with the sample. Using the $^{13}C(d,p)^{14}C$ reaction, it was possible for us to follow and quantify the ^{13}C distribution at the micrometric scale along the nanotube carpets.

In Figure 1, SEM micrographs of classical sample A are reported, showing that there are almost no byproducts (amorphous carbon, metal particles, etc.) and that nanotubes are mainly aligned as in a carpet (Figure 1a). The height of the carpet, that is, nanotube length, reaches 500 μm; the mean growth rate is thus 30 μm/min. This high growth rate is constant regardless of the synthesis duration in the 2−30 min range. In addition, these micrographs show that purity and alignment are varying along the carpet height. The base of the carpet (Figure 1c) (in contact with the Si substrate) is clean, and nanotubes are oriented in the same direction. In the core of the carpet, nanotubes appear well aligned (see also Figure S2). However, in the last 10 μm at the top of the carpet, nanotubes are entangled and some byproducts (particles) are occurring (Figure 1b). TEM observations (see Figure S3) show multiwalled nanotubes that are filled partially with iron nanowires in the γ phase, as determined by X-ray diffraction.[19] Taking into account the growth mechanisms described in the literature,[9,12,15] a first analysis of our observations would suggest that nanotubes grow entangled at the end of the synthesis process. However, this result raises the question of nanotube growth chronology during carpet formation.

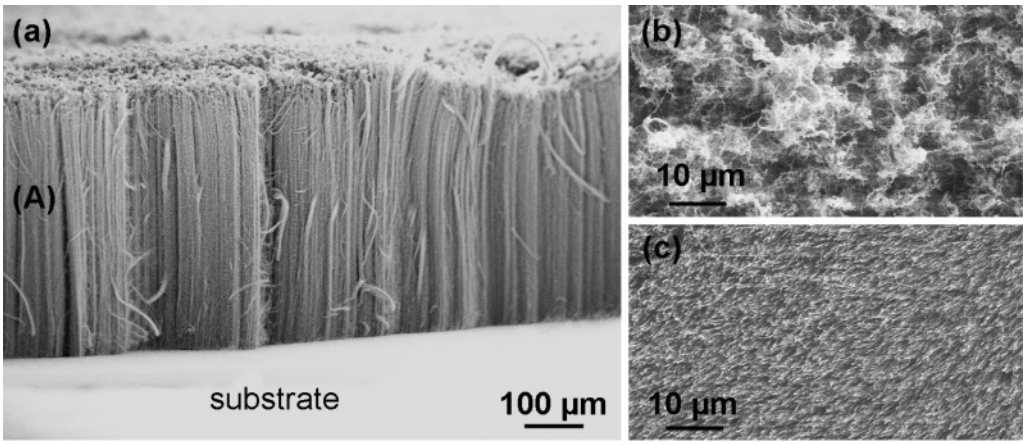

Figure 1. SEM images of (a) the cross-section of a typical carpet of aligned carbon nanotubes (sample A), (b) the top of carpet A, and (c) the base of carpet A after scratching from the substrate.

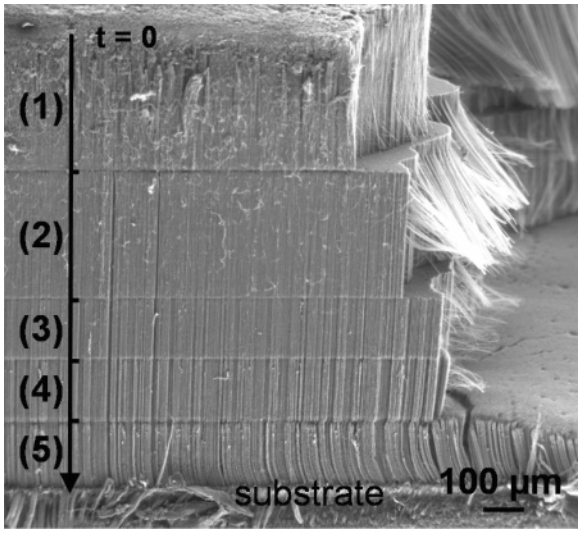

Figure 2. SEM images of the cross sections of multilayered carpet P1; the numbers on each layer correspond to the number of injection sequences reported in Table 1.

Figures 2−4 report SEM observations of samples obtained with the sequential synthesis procedure and reveal a first interesting result: samples P1 (Figure 2), P2 (Figure 3), I1, and I2 (Figure 4) are composed of several stacked carpets constituting a multilayered deposit on an Si substrate. For the P1 sample (Figure 2) synthesized from sequential injections of the same solution but of different durations, the number of carpets corresponds to the number of injections (see also Table S1). Considering that the nanotube growth rate is constant (ca. 30 μm/min), it is then possible to localize the layer corresponding to each injection. In Figure 2, it is possible to distinguish five piled layers of well-aligned MWNTs: two successive layers (each 275 μm thick) are observed at the top of the multilayered carpet and three additional layers (each 140 μm thick) have grown close to the Si substrate under the former ones. Obviously, the two layers at the top correspond to the first two injections (sequences 1 and 2, Table 1), whereas the three layers at the bottom correspond to the last three injections (sequences 3−5). The same chronology in the formation of stacked carpets was observed for sample P2 (Figure 3a), which is composed of two similar layers at the top (corresponding to the two successive injection of 15 min each) and one thicker layer at the base in contact with the Si substrate (corresponding to the last injection of 20 min).

Therefore, these striking results demonstrate that the layer corresponding to the second injection sequence is systematically growing below the layer corresponding to the first

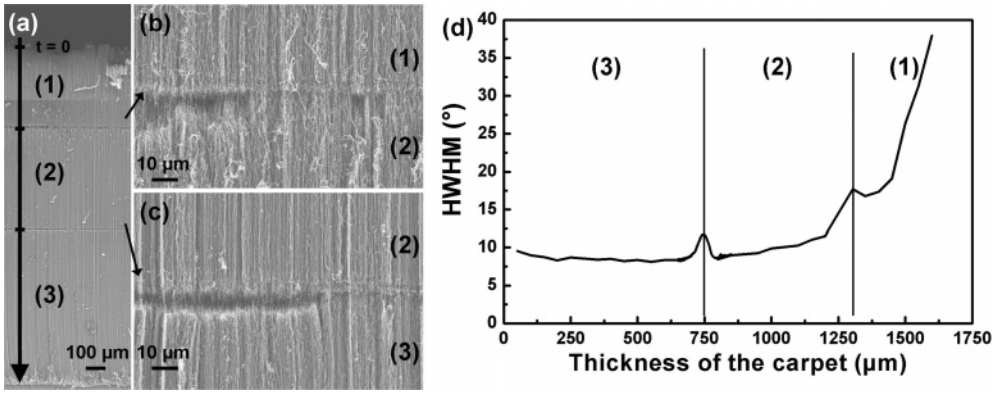

Figure 3. SEM image of (a) a cross section of sample P2 showing three stacked layers of well-aligned nanotubes (numbers 1−3 correspond to the injection sequences in Table 1), (b and c) interfaces between the different layers, and (d) XRD measurements (microbeam, ESRF, ID13) of the alignment degree of nanotubes as a function of carpet thickness.

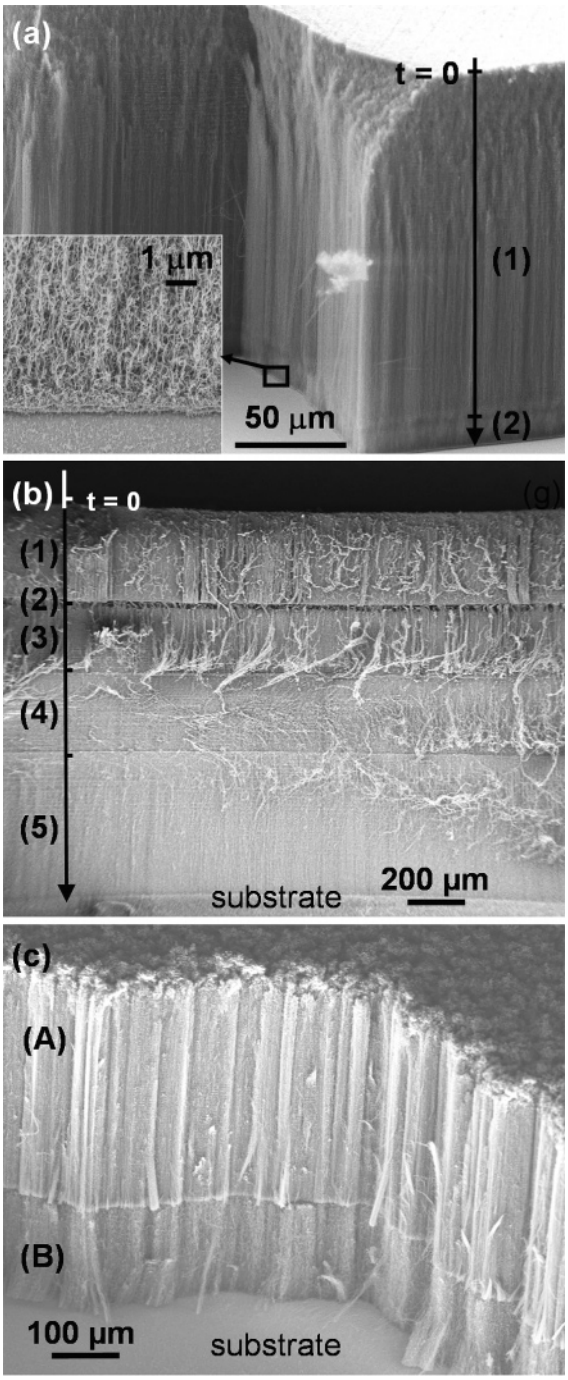

Figure 4. SEM images of the cross sections of multilayered carpets: (a) sample I1 composed of one carpet over a thin layer of disordered carbon (micrograph magnified at the bottom), (b) sample I2 composed of 4 stacked layers, and (c) sample P3 composed of a new layer B growing under the typical carpet, A. The numbers on each picture correspond to the numbering of injection sequences reported in Table 1.

injection sequence, namely, between the substrate and the first layer. This phenomenon is reproducible for all of the other successive injections: the last sequence always gives rise to the layer in contact with the substrate. In addition, it is important to note that the surface and the base of the multilayered carpets are similar to those observed on a simple carpet (Figure 1b and c). Each layer can be easily separated from the others, and between each layer the nanotube alignment does not look as good as that in the carpet core. A thin interface of a few micrometers where nanotubes are entangled can be observed (Figure 3b and c), showing disruption of the nanotube alignment and sometimes separation between the layers. Analysis of X-ray microdiffraction experiments performed on sample P2 (Figure 3d) demonstrates that the nanotube alignment degree is better for the last grown layer (close to the substrate) as compared to the first grown ones and the alignment is disrupted at the interface between two layers. Therefore, entangled nanotubes are always occurring at the top of each carpet. In addition, we observed such nanotube arrangement already during the early stages of nanotube growth.[16,18] These observations demonstrate that the layer of entangled nanotube is first formed and is lifted up during nanotube growth. On the contrary, the base of the carpet or of the multilayered carpet is composed of the last grown walls of nanotubes. All of these results give strong evidence that nanotubes are always growing directly on the substrate surface and not on the top of the pre-existing carpet as was often suggested in the literature.[12,15] In addition, the base-growth mechanism, identified during the early stages of nanotube growth,[16] is still occurring all along the formation of the carpet.

For samples I1 and I2 (Figure 4a and b), synthesized from sequenced injection of different solutions (containing or not ferrocene), the chronology of the formation of the stacked carpets is similar to the one observed for samples P1 and P2. However, the number of stacked carpets is not corresponding to the number of injection sequences. Indeed, the injection of a solution without ferrocene does not induce any aligned nanotube carpet formation. Only a very thin layer of disordered carbon can be observed. In particular, sample I1 (Figure 4a) exhibits a 20-μm-thick layer in contact with the substrate and composed of few nanotubes embedded in amorphous carbon structures. This indicates that during the second injection, of 12 min, corresponding to toluene aerosol (no ferrocene), almost no nanotubes grow. However, for sample I2 (Figure 4b), as soon as new injections with ferrocene start (injections 3−5), nanotubes start to grow again from the surface of the substrate, under the disordered carbon layer, forming new aligned MWNT layers. These results demonstrate the important role of the continuous feeding of ferrocene for the continuous and fast growth of aligned carbon nanotubes and suggest that the catalyst originating nanotube growth is playing its role mainly on the surface substrate. They also give evidence that a new layer can grow even under a layer that does not contain aligned nanotubes.

For sample P3, the injection of toluene/ferrocene solution during a 10-min time period on carpet A previously grown on an Si substrate (Figure 1a) involves the formation of a 150-μm-high carpet (B) directly on the Si substrate, under carpet A (Figure 4c). This result demonstrates that it is possible to grow a carpet directly on an Si substrate under a pre-existing one already synthesized and stored at room temperature.

Sample I3, obtained from four injection sequences of either standard benzene/ferrocene solution or ^{13}C-enriched solution without stopping between each injection, does not exhibit a

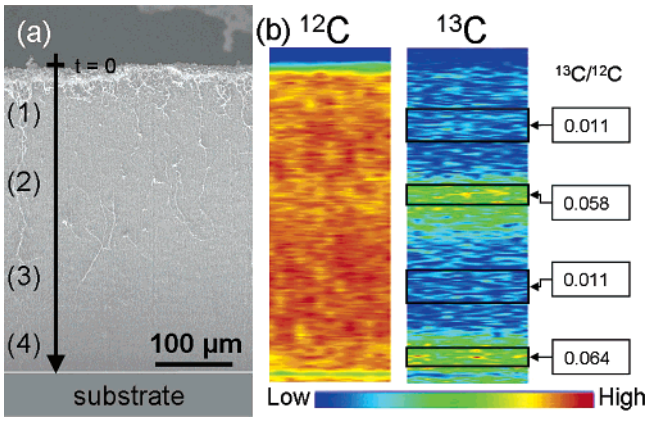

Figure 5. (a) SEM image of a cross section of sample I3 showing only one layer of aligned MWNTs. (b) ^{12}C and ^{13}C mapping of sample I3 showing four separated regions with different $^{13}C/^{12}C$ ratios.

multilayered morphology. No stacked carpets can be distinguished, only a 400-μm-thick layer can be observed (Figure 5 a). However, the carbon mapping along the carpet height obtained with a nuclear microprobe (Figure 5b) reveals that this carpet is composed of four stacked parts; each of them can be distinguished by the ^{13}C enrichement level. The stacking order of each part follows the chronology of the injection sequences closely: parts 1 and 3 exhibit a $^{13}C/^{12}C$ ratio similar to the one in natural carbon, thus corresponding to the injections of standard benzene/ferrocene solution, whereas parts 2 and 4 exhibit a higher $^{13}C/^{12}C$ ratio, thus corresponding to injection of ^{13}C-enriched benzene/ferrocene solution. This stacking order confirms the chronology described for all of the above samples and is consistent with another carbon monitoring study performed in CVD of gaseous hydrocarbon.[5] In our case, it is noteworthy that the $^{13}C/^{12}C$ ratio is always 0.06 in ^{13}C-enriched parts and 0.01 in nonenriched parts. This is attesting that there is no ^{13}C deposition on the pre-existing carpet and there is no carbon migration along the nanotube walls.

Therefore, C mapping gives strong and definitive evidence that carbon species diffuse through the whole carpet thickness and subsequently feed the origin of the nanotube growth located on the surface substrate. The feeding of both carbon and the catalytic source (ferrocene) in the reactor during the aerosol-assisted CCVD process involves the continuous catalytic decomposition of toluene and then the diffusion of the reactive C species through the whole carpet. Subsequently, formation of graphene sheets on catalytic particles located on the Si substrate[16] is occurring, thus allowing the continuous growth of the carpet or generating a new carpet under the pre-existing one through a base-growth mechanism.

Our results demonstrate that the analysis of multilayered carpets of aligned MWNTs obtained by sequential synthesis is an efficient way to evidence the growth mechanisms experimentally. The growth chronology was established. The growth of a new layer always occurs directly on the substrate surface, under the pre-existing layers by lifting them up, thus involving a base-growth mechanism all along carpet formation. The formation of a proper layer on a surface substrate is stopped only when ferrocene is not fed in the reactor, attesting the important role of catalyst continuous feeding on the continuous nanotube growth. In addition, as soon as ferrocene is fed again, a new aligned nanotube layer is growing under the pre-existing ones, suggesting that the catalyst originating the growth is acting only on the surface substrate. This study enables one to definitely establish carbon progress all along aligned carbon nanotube formation. Regarding catalyst progress, the first indications obtained here will be completed by catalyst monitoring experiments.

Acknowledgment. We gratefully acknowledge Dominique Porterat and Daniel Crozat for efficient technical support, Sylvie Poissonnet and Patrick Bonnaillie for assistance in SEM observations, and Manfred Burghammer and Christian Rieckel for technical assistance and fruitful scientific discussions during X-ray diffraction experiments at ESRF. The FIT2D program provided by A. P. Hammersley and the ESRF was used for the X-ray data analysis.

Supporting Information Available: The experimental setup (Figure S1), a high-magnification SEM micrograph of the core of a typical carpet showing well-aligned nanotubes (Figure S2), a typical TEM picture showing multiwalled nanotubes partly filled with iron (Figure S3), and the thickness of the layers in the multilayered samples (Table S1). This material is available free of charge via the Internet at http://pubs.acs.org.

References

(1) Iijima, S. *Nature* **1991**, *354*, 56−58.
(2) Li, W. Z.; Xie, S. S.; Qian, L. X.; Chang, B. H.; Zou, B. S.; Zhou, W. Y.; Zhao, R. A.; Wang, G. *Science* **1996**, *274*, 1701−1703.
(3) Ren, Z. F.; Huang, Z. P.; Xu, J. W.; Wang, J. H.; Bush, P.; Siegal, M. P.; Provencio, P. N. *Science* **1998**, *282*, 1105−1107.
(4) Huang, S.; Dai, L.; Mau, A. W. H. *J. Phys. Chem. B* **1999**, *103*, 4223−4227.
(5) Fan, S. F.; Liu, L.; Liu, M. *Nanotechnology* **2003**, *14*, 1118−1123.
(6) Sinnott, S. B.; Andrews, R.; Qian, D.; Rao, A. M.; Mao, Z.; Dickey, E. C.; Derbyshire, F. *Chem. Phys. Lett.* **1999**, *315*, 25−30.
(7) Kamalakaran, R.; Terrones, M.; Seeger, T.; Kohler-Redlich, P.; Rülhe, M.; Kim, Y. A.; Hayashi, T.; Endo, M. *Appl. Phys. Lett.* **2000**, *77*, 3385−3387.
(8) Mayne, M.; Grobert, N.; Terrones, M.; Kamalakaran, R.; Rühle, M.; Kroto, H. W.; Walton, D. R. M. *Chem. Phys. Lett.* **2001**, *338*, 101−107.
(9) Zhang, X.; Cao, A.; Wei, B.; Li, Y.; Wei, J.; Xu, C.; Wu, D. *Chem. Phys. Lett.* **2002**, *362*, 285−290.
(10) Singh, C.; Shaffer, M. S. P.; Windle, A. H. *Carbon* **2003**, *41*, 359−368.
(11) Dell'Acqua-Bellavitis, L. M.; Ballard, J. D.; Ajayan, P. M.; Siegel, R. W. *Nano Lett.* **2004**, *4*, 1613−1620.
(12) Cao, A.; Zhang, X.; Wei, J.; Li, Y.; Xu, C.; Liang, J.; Wu, D.; Wei, B. *J. Phys. Chem. B* **2001**, *105*, 11937−11940.
(13) Zhang, X.; Cao, A.; Li, Y.; Xu, C.; Liang, J.; Wu, D.; Wei, B. *Chem. Phys. Lett.* **2002**, *351*, 183−188.
(14) Zhang, H.; Liang, E.; Ding, P.; Chao, M. *Physica B* **2003**, *337*, 10−16.
(15) Deck, C. P.; Vecchio, K. S.; *J. Phys. Chem. B* **2005**, *109*, 12353−12357.
(16) Pinault, M.; Mayne-L'Hermite, M.; Reynaud, C.; Pichot, V.; Launois, P.; Ballutaud, D. *Carbon* **2005**, *43*, 2968−2976.
(17) Mayne-L'Hermite, M.; Armand, X.; Porterat, D.; Reynaud, C. In *Proceedings of the Chemical Vapor Deposition-XVI and EUROCVD-14*; Allendorf, M., Maury, F., Teyssandier, F., Eds., 2003; Vols. 2003−2008, pp 549−556.
(18) Pinault, M.; Mayne-L'Hermite, M.; Reynaud, C.; Beyssac, O.; Rouzaud, J. N.; Clinard, C. *Diamond Relat. Mater.* **2004**, *13*, 1266−1269.
(19) Pichot, V.; Launois, P.; Pinault, M.; Mayne-L'Hermite, M.; Reynaud, C. *Appl. Phys. Lett.* **2004**, *85*, 473−475.

NL051472K